

**Particle segregation by Stokes number for small neutrally buoyant spheres in a fluid**

Phanindra Tallapragada\* and Shane D. Ross†

*Department of Engineering Science and Mechanics, Virginia Polytechnic Institute and State University, (VPISU), Blacksburg, VA 24061, USA*

(Received 12 March 2008; revised manuscript received 14 June 2008; published 10 September 2008)

It is a commonly observed phenomenon that spherical particles with inertia in an incompressible fluid do not behave as ideal tracers. Due to the inertia of the particle, the planar dynamics are described in a four-dimensional phase space and thus can differ considerably from the ideal tracer dynamics. Using finite-time Lyapunov exponents, we compute the sensitivity of the final position of a particle with respect to its initial velocity, relative to the fluid, and thus partition the relative velocity subspace at each point in configuration space. The computations are done at every point in the relative velocity subspace, thus giving a sensitivity field. The Stokes number, being a measure of the independence of the particle from the underlying fluid flow, acts as a parameter in determining the variation in these partitions. We demonstrate how this partition framework can be used to segregate particles by Stokes number in a fluid. The fluid model used for demonstration is a two-dimensional cellular flow.

DOI: [10.1103/PhysRevE.78.036308](https://doi.org/10.1103/PhysRevE.78.036308)

PACS number(s): 47.52.+j, 47.51.+a

**I. INTRODUCTION**

It has long been observed that particles with a finite size and mass have different dynamics from the ambient fluid. Because of their inertia the particles do not evolve as point-like tracers in a fluid. This leads to preferential concentration, clustering, and separation of particles as observed in numerous studies [1–3]. The inertial dynamics of solid particles can have important implications in natural phenomena, e.g., the transport of pollutants and pathogenic spores in the atmosphere [4,5], formation of rain clouds [6] by coalescence around dust particles, and formation of plankton colonies in oceans [7]. Similarly, the inertial dynamics of reactant particles is important in the reaction kinetics and distribution of reactants in solution for coalescence-type reactions [8]. Mixing-sensitive reactions in the wake of bubbles have been shown to be driven by buoyancy effects of reactants [9]. Recently, a principle of asymmetric bifurcation of laminar flows was applied to the separation of particles by size and demonstrated the separation of flexible biological particles and the fractional distillation of blood [10,11]. Innovative channel geometries have been empirically designed to focus randomly ordered inertial particles in microchannels [12]. These phenomena and related applications rely on the non-trivial dynamics of inertial particles in a fluid.

Many theoretical and numerical studies have been done on the dynamics of inertial particles in some model flows, using the Maxey-Riley equation [13]. Maxey [14] studied the settling properties and retention zones of nonbuoyant inertial particles in vertical cellular flows, under the influence of gravity. The sensitive dependence on the initial conditions of inertial particle trajectories and clustering was further studied by [15] using a two-dimensional cellular flow for neutrally buoyant particles.

Several studies have been concerned with characterizing the surface in physical space to which inertial particles clus-

ter, using, for instance, fractal dimension and rates of convergence to this surface. Among these, [16–18] studied clustering of inertial particles in two-dimensional flow past a cylinder. Similar studies [19–22] considered inertial particle clustering in turbulent flows. In the turbulent flow studies, the spectrum of (long-time) Lyapunov exponents was computed to calculate the fractal dimension of the surfaces of particle clustering. While we also use Lyapunov exponents, we use them in a different way, as described below.

A method to segregate inertial particles from an initial mixture by different sizes (i.e., Stokes numbers) was numerically demonstrated in [23], but no physical description was given of how segregation arose. We provide a description by partitioning phase space into zones of initial phase space locations where inertial particles will evolve to different final locations, according to Stokes number. To achieve this, we calculate the phase space distribution of short-time Lyapunov exponents, and use topological features of this distribution to find the partition boundaries. This partition is parametrized by the Stokes number. We demonstrate this method using a simple test model of two-dimensional flow, namely, cellular flow, demonstrating that this partitioning scheme can explain the sensitive dependence of trajectories on initial conditions and the consequent clustering effects. We argue that this methodology can be used as a systematic tool to achieve segregation of inertial particles in a fluid.

We employ a simplified form of the Maxey-Riley equation [13] as the governing equation for the motion of inertial particles in a fluid. The dynamics of a single particle occur in a four-dimensional phase space. The sensitive dependence of the particle motion on initial conditions is quantified using the finite-time Lyapunov exponents (FTLEs). It has been shown previously [24,25], that the ridges in the FTLE field act as separatrices. These are in general time dependent and go by the name of Lagrangian coherent structures (LCSs). We chose to do a simplified sensitivity analysis by perturbing the initial conditions in only two dimensions, in the initial relative velocity subspace. We obtain a sensitivity field akin to a FTLE field but restricted to the relative velocity subspace, and demonstrate numerically that the ridges in this

\*tssap@vt.edu

†sdross@vt.edu

field act as separatrices. The partitions in the relative velocity subspace created by these separatrices determine the eventual spatial distribution of particles in the fluid. Using this partitioning scheme we show how the Stokes number acts as a parameter in the separation of particles of different inertia or size.

The paper is organized as follows. In Sec. II we review the equation governing the inertial particle dynamics in a fluid and its simplified form. In Sec. III we briefly review the background theory of phase space distributions of finite-time Lyapunov exponents, which we use to quantify the sensitivity of the physical location of inertial particles with respect to perturbations in the initial relative velocity. We also describe our computational scheme to obtain the sensitivity field in the relative velocity subspace. In Sec. IV we present results for the sensitivity field of the inertial particles in a cellular flow. In Sec. V we demonstrate our procedure for the segregation of particles by their Stokes number using the results from Sec. IV. In Sec. VI we give numerical justification for the robustness of the sensitivity field to perturbations in the velocity field of the fluid. In Sec. VII we discuss the results and give conclusions.

## II. GOVERNING EQUATIONS

Our starting point is Maxey and Riley's equation of motion of a rigid spherical particle in a fluid [13]:

$$\begin{aligned} \rho_p \frac{d\mathbf{v}}{dt} = & \rho_f \frac{D\mathbf{u}}{Dt} + (\rho_p - \rho_f)\mathbf{g} - \frac{9\nu\rho_f}{2a^2} \left( \mathbf{v} - \mathbf{u} - \frac{a^2}{6}\nabla^2\mathbf{u} \right) \\ & - \frac{\rho_f}{2} \left[ \frac{d\mathbf{v}}{dt} - \frac{D}{Dt} \left( \mathbf{u} - \frac{a^2}{10}\nabla^2\mathbf{u} \right) \right] \\ & - \frac{9\rho_f}{2a} \sqrt{\frac{\nu}{\pi}} \int_0^t \frac{1}{\sqrt{t-\tau}} \frac{d}{d\tau} \left( \mathbf{v} - \mathbf{u} - \frac{a^2}{6}\nabla^2\mathbf{u} \right) d\tau, \end{aligned} \quad (1)$$

where  $\mathbf{v}$  is the velocity of the solid spherical particle,  $\mathbf{u}$  the velocity field of the fluid,  $\rho_p$  the density of the particle,  $\rho_f$  the density of the fluid,  $\nu$  the kinematic viscosity of the fluid,  $a$  the radius of the particle, and  $\mathbf{g}$  the acceleration due to gravity. The terms on the right-hand side are the force exerted by the undisturbed flow on the particle, the force of buoyancy, the Stokes drag, the added mass correction, and the Basset-Boussinesq history force, respectively. Equation (1) is valid under the following restrictions:

$$\begin{aligned} a(\mathbf{v} - \mathbf{u})/\nu & \ll 1, \\ a/L & \ll 1, \\ \left( \frac{a^2}{\nu} \right) \left( \frac{U}{L} \right) & \ll 1, \end{aligned} \quad (2)$$

where  $L$  and  $U/L$  are the length scale and velocity gradient scale for the undisturbed fluid flow. The derivative

$$\frac{D\mathbf{u}}{Dt} = \frac{\partial\mathbf{u}}{\partial t} + (\mathbf{u} \cdot \nabla)\mathbf{u} \quad (3)$$

is the acceleration of a fluid particle along the fluid trajectory, whereas the derivative

$$\frac{d\mathbf{v}}{dt} = \frac{\partial\mathbf{v}}{\partial t} + (\mathbf{v} \cdot \nabla)\mathbf{v} \quad (4)$$

is the acceleration of a solid particle along the solid particle trajectory.

Equation (1) can be simplified by neglecting the Faxen correction and the Basset-Boussinesq terms [15]. We restrict our study to the case of neutrally buoyant particles, i.e.,  $\rho_p = \rho_f$ . Writing  $\mathbf{W} = (\mathbf{v} - \mathbf{u})$ , the relative velocity of the particle and the surrounding fluid, the evolution of  $\mathbf{W}$  becomes

$$\frac{d\mathbf{W}}{dt} = -(J + \mu I)\mathbf{W}, \quad (5)$$

and the change in the particle position is given by

$$\frac{d\mathbf{r}}{dt} = \mathbf{W} + \mathbf{u}, \quad (6)$$

where  $J$  is the gradient of the undisturbed velocity field of the fluid,  $\mathbf{r} = (x, y)$  is the position of the solid particle, and  $\mu = \frac{2}{3}\text{St}^{-1}$  is a constant for a particle with a given Stokes number  $\text{St}$ . Equations (5) and (6) can be rewritten as the vector field

$$\frac{d\xi}{dt} = \mathbf{F}(\xi), \quad (7)$$

with  $\xi = (\mathbf{r}, \mathbf{W}) = (x, y, W_x, W_y) \in \mathbb{R}^4$ . Equation (7) defines a dissipative system with constant divergence  $-\frac{4}{3}\mu$ . It has been shown by Haller [17] that an exponentially attracting slow manifold exists for general unsteady inertial particle motion as long as the particle Stokes number is small enough. For neutrally buoyant particles this attractor is  $\mathbf{W} = \mathbf{0}$  (the  $xy$  plane). Despite the global attractiveness of the slow manifold, domains of instability exist in which particle trajectories diverge [15,16,18].

## III. SENSITIVITY ANALYSIS

The Lyapunov characteristic exponent is widely used to quantify the sensitivity to initial conditions. A positive Lyapunov exponent is a good indicator of chaotic behavior. We have used the finite-time version of the Lyapunov exponents, the FTLEs, as a measure of the maximum stretching for a pair of phase points.

We review some important background regarding the FTLEs below, following [24–26]. The solution to Eq. (7) can be given by a flow map  $\phi_{t_0}^t$ , which maps an initial point  $\xi(t_0)$  at time  $t_0$  to  $\xi(t)$  at time  $t$ ,

$$\xi(t) = \phi_{t_0}^t(\xi(t_0)). \quad (8)$$

The evolution over a time  $T$  of the displacement between two initially close phase points  $\xi(t_0)$  and  $\xi(t_0) + \delta\xi(t_0)$  is given by

$$\delta\xi(t_0 + T) = \frac{d\phi_{t_0}^{t_0+T}(\xi)}{d\xi} \delta\xi(t_0) + O(\|\delta\xi\|^2). \quad (9)$$

Neglecting the higher-order terms, the magnitude of the perturbation is

$$\|\delta\xi(t_0 + T)\| = \sqrt{\left\langle \delta\xi(t_0), \frac{d\phi_{t_0}^{t_0+T}(\xi)^*}{d\xi} \frac{d\phi_{t_0}^{t_0+T}(\xi)}{d\xi} \delta\xi(t_0) \right\rangle}. \quad (10)$$

The matrix

$$C = \frac{d\phi_{t_0}^{t_0+T}(\xi)^*}{d\xi} \frac{d\phi_{t_0}^{t_0+T}(\xi)}{d\xi} \quad (11)$$

is the right Cauchy-Green deformation tensor. Maximum stretching occurs when the perturbation  $\delta\xi$  is along the eigenvector  $\mathbf{n}_{\max}$  corresponding to the maximum eigenvalue  $\lambda_{\max}$  of  $C$ . The growth ratio is given by

$$\|\delta\xi(t_0 + T)\| / \|\delta\xi(t_0)\| = e^{\sigma_1(\xi(t_0))|T|}, \quad (12)$$

where

$$\sigma_1(\xi(t_0)) = \frac{1}{|T|} \ln \sqrt{\lambda_{\max}(C)} \quad (13)$$

is the maximal finite-time Lyapunov exponent. One can associate an entire spectrum of finite-time Lyapunov exponents with  $\xi(t_0)$ , ordering them as

$$\sigma_1(\xi(t_0)) > \sigma_2(\xi(t_0)) > \sigma_3(\xi(t_0)) > \sigma_4(\xi(t_0)). \quad (14)$$

The entire spectrum of the Lyapunov exponents can be computed from the state transition  $\Phi(t, t_0) = d\phi_{t_0}^t(\xi)/d\xi$  matrix using singular value decomposition, where  $t = t_0 + T$ ,

$$\Phi(t, t_0) = B(t, t_0) \Lambda(t, t_0)^{1/2} R(t, t_0). \quad (15)$$

The diagonal matrix  $\Lambda$  gives all the Lyapunov exponents while

$$\Sigma(t_f, t_0) = \ln[\Lambda(t_f, t_0)^{1/2|T|}], \quad (16)$$

where  $T = t_f - t_0$  and  $\Sigma(t_f, t_0) = \text{diag}(\sigma_1, \dots, \sigma_4)$ . An arbitrary perturbation in the fixed basis can be transformed using a time-dependent transformation [26]

$$\delta\xi'(t) = A(t, t_0, t_f) \delta\xi(t), \quad (17)$$

such that in the new basis (the primed frame), the variational equations become

$$\delta\xi'(t) = \Sigma(t_f, t_0) \delta\xi'(t). \quad (18)$$

Since  $\Sigma(t_f, t_0)$  is a constant diagonal matrix, we have

$$\delta\xi'(t) = e^{(t-t_0)\Sigma(t_f, t_0)} \delta\xi'(t_0). \quad (19)$$

The first coordinate in the new frame grows as  $\delta\xi'_1(t) = e^{(t-t_0)\sigma_1} \delta\xi'_1(t_0)$ . The time-dependent transformation  $A(t)$  is given by [26]

$$A(t, t_0, t_f) = e^{(t-t_0)\Sigma(t_f, t_0)} R(t_f, t_0)^* R(t, t_0) \Sigma(t, t_0)^{-1/2} B(t, t_0). \quad (20)$$

### A. Sensitivity to initial relative velocity

Since the dynamics of the inertial particle is in a four-dimensional phase space, the separatrices, that is, LCSs defined by ridges in the field of the maximal FTLEs, are three-dimensional surfaces (see [25]). However, because the system is dissipative and the global attractor is the  $xy$  subspace, we can obtain meaningful information by restricting the computations to a lower-dimensional subdomain of the phase space. This we do by considering an initial perturbation only in the relative velocity subspace and study how this perturbation grows in the  $xy$  plane, the configuration space, i.e.,

$$\delta\xi(t_0) = [0, 0, \Delta W_x, \Delta W_y]^*, \quad (21)$$

where  $\Delta W_x$  and  $\Delta W_y$  are the perturbations in the relative velocity subspace. It is to be noted that when perturbations are applied to the initial velocity of the solid particle, an initial drag is experienced by the particle, but this effect is negligible [14].

Using the time-dependent transformation  $A(t, t_0, t_f)$  the evolution of the perturbation is given by

$$\delta\xi(t) = A^{-1}(t) e^{(t-t_0)\Sigma(t_f, t_0)} A(t_0) \delta\xi(t_0). \quad (22)$$

The growth of perturbations in the  $xy$  plane is given by the first two components of the above vector. The last two components are the evolution of the perturbations in the relative velocity subspace. Since the  $xy$  plane is a global attracting set, these tend to zero. One can choose a finite time  $T$  such that the evolution of the initial perturbation comes arbitrarily close to the  $xy$  plane. In this way the sensitivity of the final spatial location of the particles with respect to initial relative velocity can be computed.

### B. Numerical computation of the sensitivity field

The evolution of a perturbation is along the four basis vectors. For an arbitrarily oriented initial perturbation the growth may not be dominated in the direction of greatest expansion for short integration times. This can be overcome by sampling multiple perturbations in the different directions. A reference point and its neighbors are identified and after a finite time their positions in configuration space are

computed. The state transition matrix can then be computed at each point in the  $xy$  plane, by using a central finite-

difference method. For initial perturbations restricted to  $W_x W_y$  subspace, this gives

$$\Phi_{,rW} = \begin{pmatrix} \frac{x_{i,j,k+1,l}(t_0+T) - x_{i,j,k-1,l}(t_0+T)}{\Delta W_x(t_0)} & \frac{x_{i,j,k,l+1}(t_0+T) - x_{i,j,k,l-1}(t_0+T)}{\Delta W_y(t_0)} \\ \frac{y_{i,j,k+1,l}(t_0+T) - y_{i,j,k-1,l}(t_0+T)}{\Delta W_x(t_0)} & \frac{y_{i,j,k,l+1}(t_0+T) - y_{i,j,k,l-1}(t_0+T)}{\Delta W_y(t_0)} \end{pmatrix}. \quad (23)$$

In the four-dimensional finite-difference grid (indexed by  $i, j, k, l$ ), each reference point has eight neighboring points, one along each of the positive and negative directions in each phase space direction. Since we are looking at the initial perturbations in relative velocity only, we fix the initial spatial position of the particle ( $i, j$ ) but vary its relative velocity ( $k, l$ ). In the relative velocity, points are separated by constant amounts  $\Delta W_x, \Delta W_y$  in the  $x, y$  relative velocity directions, respectively.

The relative velocity sensitivity field  $\sigma(W_x, W_y)$  is given by

$$\sigma(W_x, W_y) = \frac{1}{|T|} \ln \sqrt{\lambda_{\max}(\Phi_{,rW}^* \Phi_{,rW})}. \quad (24)$$

Ridges on this sensitivity surface are one dimensional structures similar to LCSs. The ridges in the maximal sensitivity field  $\sigma(W_x, W_y)$  partition the relative velocity subspace. We applied the above procedure to a cellular flow.

We make a note on the terminology used here. The field measuring the sensitivity of the final location of particles in configuration space with respect to perturbations in initial relative velocity is analogous to the FTLE field, but not identical. To obtain the true FTLE field, one would have to compute the  $4 \times 4$  state transition matrix  $\Phi$ . Using the notation of Eq. (23),

$$\Phi = \begin{pmatrix} \Phi_{,rr} & \Phi_{,rW} \\ \Phi_{,Wr} & \Phi_{,WW} \end{pmatrix}. \quad (25)$$

The FTLE field is then given by  $\sigma(x, y, W_x, W_y) = (1/|T|) \ln \sqrt{\lambda_{\max}(\Phi^* \Phi)}$ . Ridges in this field are three-dimensional structures and represent the true LCSs. Ridges in the relative velocity sensitivity field  $\sigma(W_x, W_y)$  are one-dimensional structures which can be considered “slices” of the full three-dimensional structure, where the slices are parametrized by the two-dimensional location of the initial spatial point  $(x, y)$ .

#### IV. EXAMPLE FLUID MODEL: CELLULAR FLOW

We demonstrate the computation of the relative sensitivity field using a simple test model of two-dimensional flow. We choose cellular flow, as it has been used in previous studies

[14,15], and is a simple example of a fluid with separatrices. This flow is described by the stream function

$$\psi(x, y, t) = a \cos x \cos y. \quad (26)$$

The velocity field is given by

$$u = -a \cos x \sin y, \quad (27)$$

$$v = a \sin x \cos y \quad (28)$$

There are heteroclinic connections from the stable and unstable manifolds of the fixed points  $(2n+1)(\pi/2)$ , shown by the arrows in Fig. 1, which are also the boundaries of the cells. These coincide with  $LCS_f$ , the LCSs for fluid particles, which have no relative velocity ( $W_x=W_y=0$ ) and evolve according to the fluid velocity field, Eqs. (27) and (28). The  $LCS_f$  is to be distinguished from the LCS of the inertial particle in the full four-dimensional phase space. By choosing initial perturbations of the form given by Eq. (21) at different points along a streamline, we follow how these perturbations grow in the  $xy$  plane by integrating the particle

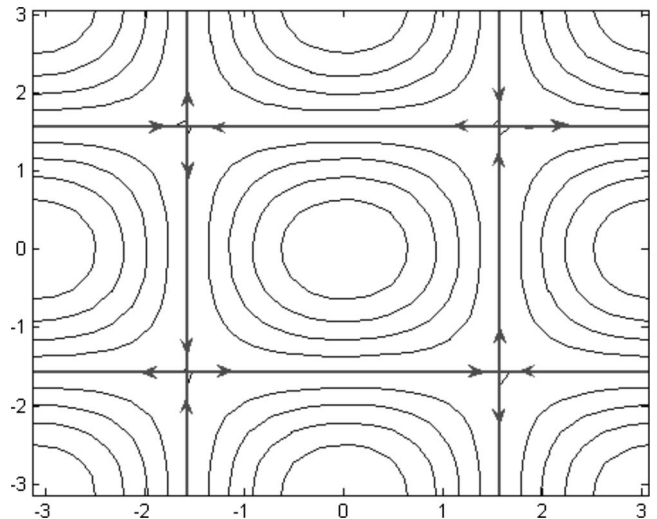


FIG. 1. Streamlines of  $\psi = a \cos x \cos y$  form an array of cells. The arrows indicate the heteroclinic fluid trajectories connecting the fixed points of the velocity field formed by  $\psi$ . For this velocity field, the heteroclinic trajectories coincide with the  $LCS_f$ , i.e., the separatrices or transport barriers, for fluid particles.

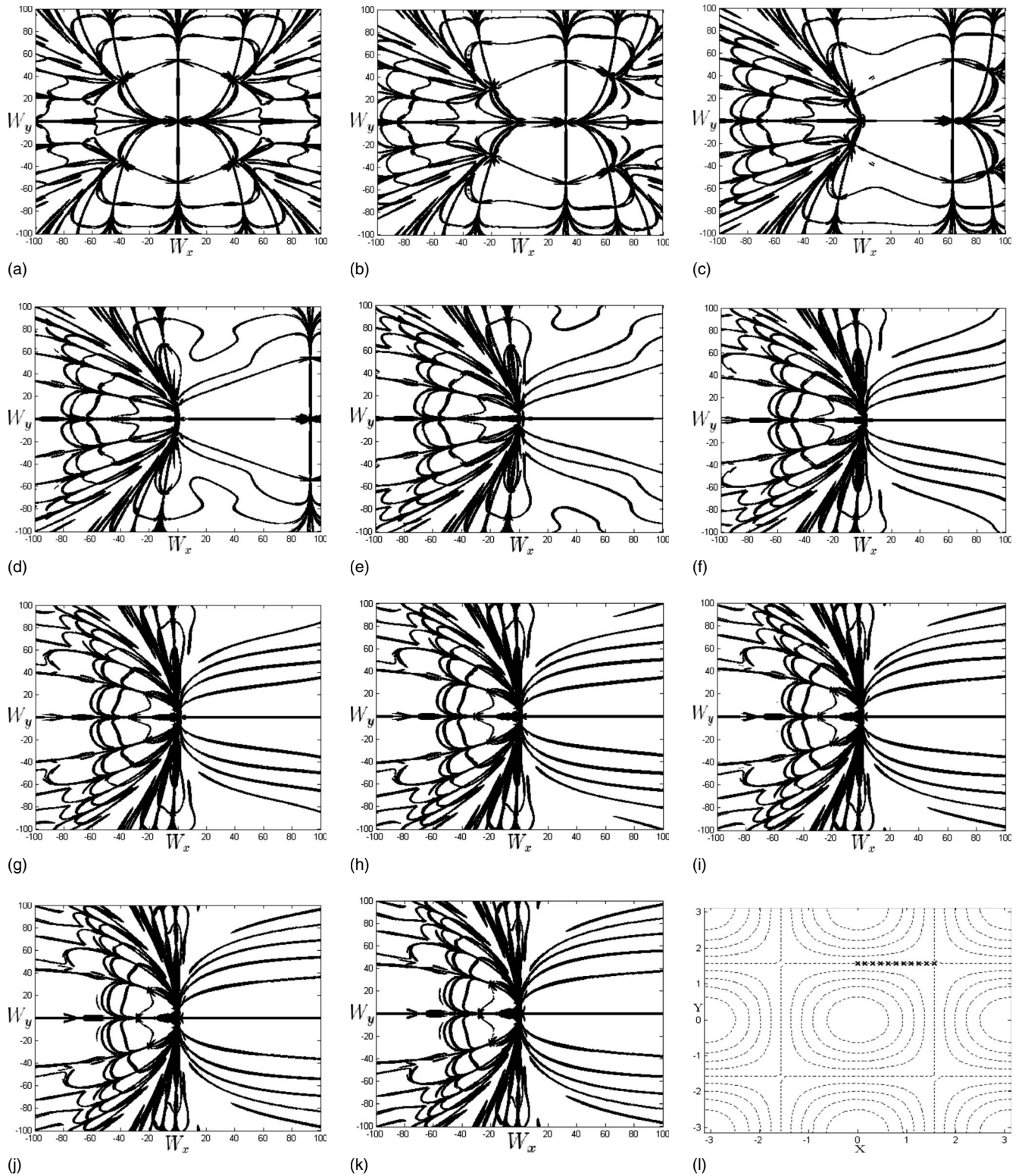


FIG. 2. Ridges in the sensitivity field for  $\psi = a \cos x \cos y$ . Initial spatial position varies from (a)  $(x_0, y_0) = (\pi/2, \pi/2)$  to (k)  $(0, \pi/2)$ , at the points shown in (l), along  $\psi = 0$ , at intervals of  $0.05\pi$ . The plots show a smooth variation in the structure of the ridges in the sensitivity field. Parameters:  $a = 100$ ,  $St = 0.2$ ,  $T = 0.24$ .

trajectories numerically from which the sensitivity field is computed. Figure 2 shows the sensitivity field computed for initial perturbations in the relative velocity subspace, at dif-

ferent points on the streamline  $\psi(x, y, t) = 0$ . The ridges in this field have high values of sensitivity. It can be seen that there is a continuous variation in the ridges of the sensitivity

field with respect to the initial  $(x, y)$  coordinates. In each case the sensitivity field at a given point depends on the underlying LCS<sub>f</sub> of the fluid flow.

The ridges in the sensitivity field have meaningful information about the dynamics of inertial particles even when computed at points far from the saddle points of the fluid flow. This is shown in Fig. 3(a) which is the sensitivity field computed at  $(x, y) = (3\pi/8, 3\pi/8)$ . The ridges in the sensitivity field partition the relative velocity subspace according to the final location of particles. In Fig. 3(b) the ridges in the sensitivity field are used to identify regions in the relative velocity subspace, which produce qualitatively different trajectories. Particles that start at the same physical location, but are in different regions of the relative velocity subspace, are neatly separated from particles that started in other regions, as shown in Fig. 3(c). Thus the ridges in the sensitivity field have the property of a separatrix.

**V. SEGREGATION OF PARTICLES BY STOKES NUMBER**

Equation (5) can be diagonalized as

$$\frac{d\mathbf{W}_d}{dt} = \begin{pmatrix} -\lambda - \mu & 0 \\ 0 & \lambda - \mu \end{pmatrix} \mathbf{W}_d, \quad (29)$$

where  $\lambda$  are the eigenvalues of the Jacobian of the fluid velocity field. If  $\mu = \frac{2}{3}St^{-1}$  is very large, then both the components of  $A_d$  will decay. For low values of  $\mu$ , one component of  $A_d$  will grow. Therefore the dynamics of an inertial particle depend on the value of  $\mu$ , that is, on the Stokes number. It is reasonable to expect that the computations of the sensitivity of the particle location to the initial relative velocity also would depend on the Stokes number. That this is indeed the case is shown by the computations of the sensitivity field for a particle with Stokes number 0.1 for the time-independent flow, as shown in Fig. 4(a). The thick lines are the ridges in the sensitivity field for particles with  $St = 0.1$  and the hatched lines are those of  $St = 0.2$ . It can be seen that, though the structure of the sensitivity field is similar, the ridges are present at different locations in the relative velocity subspace. This fact can be exploited to design a process to separate particles by their Stokes number. In this section we illustrate a simple procedure for doing this.

The ridges of the sensitivity fields computed for the two different particles of Stokes number 0.1 and 0.2, respectively, are superimposed on the same plot, as shown in Fig. 4. The subdomain of the relative velocity subspace sandwiched between the ridges of the sensitivity fields of the two types of particles forms a zone of segregation. One such sample zone is shown in gray in Fig. 4(a). Two particles, with  $St = 0.1$  and 0.2, respectively, with common initial coordinates  $(x, y) = (3\pi/8, 3\pi/8)$  and initial relative velocities belonging to the gray region, have trajectories that separate in physical space. To illustrate this, the trajectories of 500 particles of each Stokes number, starting at the same initial physical point  $(x, y) = (3\pi/8, 3\pi/8)$  and with initial relative velocities values belonging to the gray region were computed. Figures 4(b)–4(j) show snapshots of the particle positions as a function of time. The particles are completely segregated into two

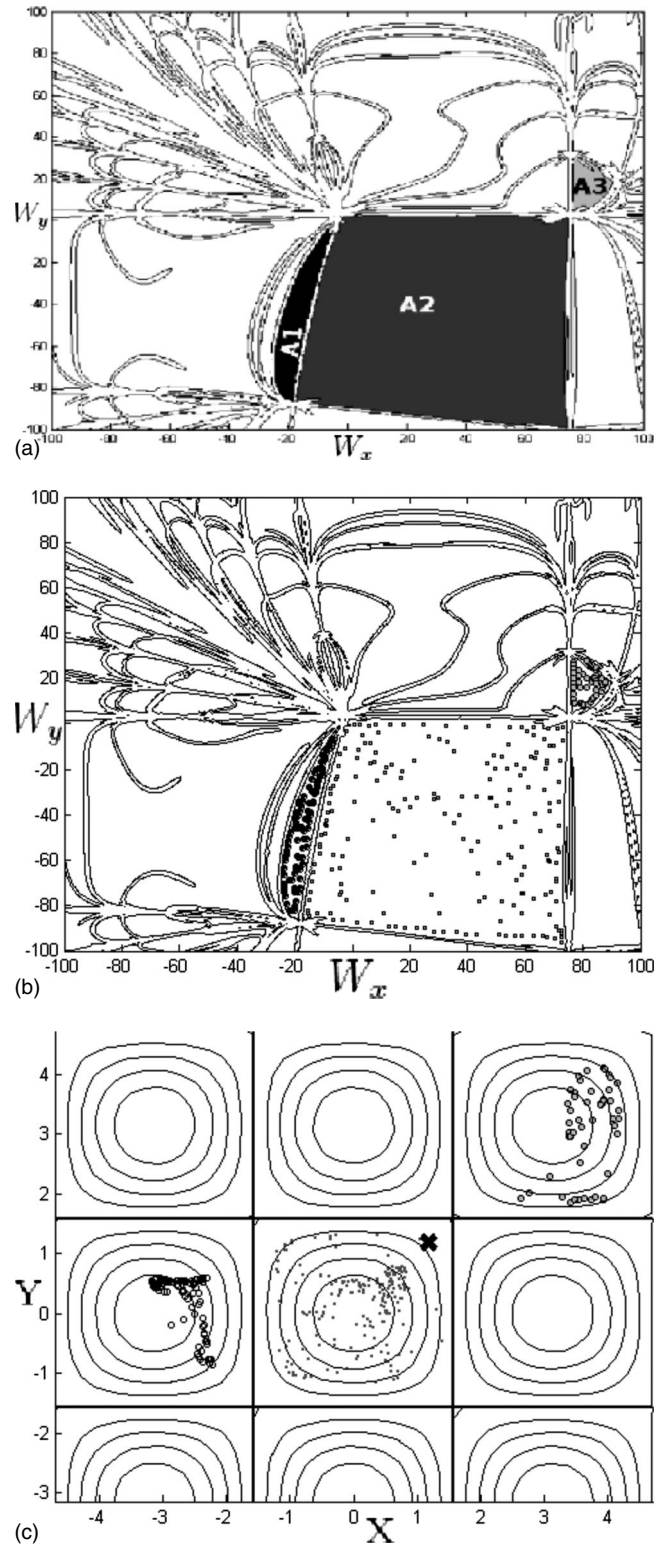


FIG. 3. (a) Ridges in the sensitivity field partition the velocity subspace into regions of distinct qualitative dynamics. Three such partitioned regions are shown. (b) Particles starting with relative initial velocities belonging to distinct partitions in the relative velocity subspace are segregated into different cells in the  $xy$  plane. Same parameters as in Fig. 2:  $a = 100$ ,  $St = 0.2$ ,  $T = 0.24$ . The initial position of all particles is  $(x_0, y_0) = (3\pi/8, 3\pi/8)$ , shown by the  $\times$  marker in (c).

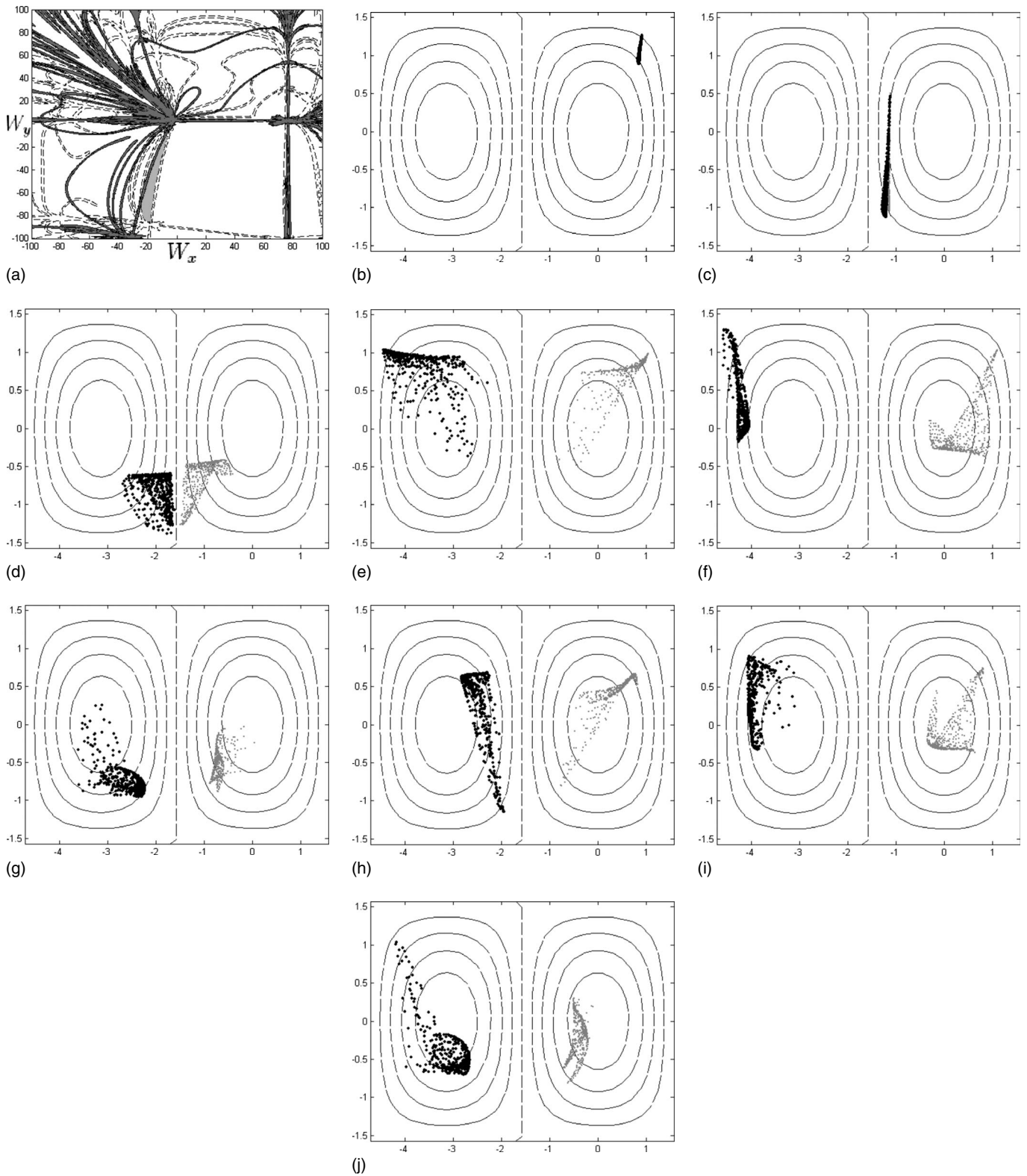


FIG. 4. (a) Ridges in the sensitivity field for particles with  $St=0.2$  (hatched) and  $St=0.1$  (thick). The initial position of all particles is  $(x_0, y_0) = (3\pi/8, 3\pi/8)$ . The gray patch is a sample region sandwiched between the ridges of the two Stokes numbers. (b)–(j) A mixture of  $St=0.1$  and  $St=0.2$  particles starting at  $(x_0, y_0) = (3\pi/8, 3\pi/8)$ , with initial relative velocity in the gray patch in (a), are separated into different cells in the  $xy$  plane after a short time.  $t =$  (b) 0.005, (c) 0.030, (d) 0.060, (e) 0.085, (f) 0.110, (g) 0.135, (h) 0.160, (i) 0.185, and (j) 0.210.

different cells after a short time ( $t \equiv 0.060$ ). Notice that the particles separate as they approach a portion of the  $LCS_f$ , the boundary of the two cells. The above procedure can be applied to any other region sandwiched between the two types of ridges and can be extended to more than two particle sizes.

**VI. ROBUSTNESS OF THE SENSITIVITY FIELD TO PERTURBATIONS IN THE STREAM FUNCTION**

The time-independent flow given by the stream function in Eq. (26) is perturbed by making it weakly time dependent. The modified fluid flow is given by the stream function [15]

$$\psi(x,y,t) = a \cos(x + b \sin \omega t) \cos y. \tag{30}$$

The velocity field is given by

$$u = -a \cos(x + b \sin \omega t) \sin y, \tag{31}$$

$$v = a \sin(x + b \sin \omega t) \cos y. \tag{32}$$

For time-varying vector fields the location of the  $LCS_f$  and LCSs depends on the choice of initial time. For the computation of the sensitivity field, the locations of ridges in the relative velocity subspace depend on the initial spatial coordinates of the particle as well as the initial time. However, our computations show that the dependence of the ridge structure on the initial time is weak. Figure 5 shows the ridges in the sensitivity field. As the initial time is increased, it is seen that there is a “squeezing” of the sensitivity field in some regions of the relative velocity subspace. A comparison of Fig. 4 with Fig. 3 shows that the ridge locations in the sensitivity field remain qualitatively the same for the three cases in Fig. 5 where the initial time is small. This offers numerical evidence that the sensitivity field is robust to small perturbations in the fluid velocity.

**VII. CONCLUSION**

The dynamics of inertial particles in a fluid flow can exhibit sensitivity to initial conditions. We demonstrated that ridges in the relative velocity sensitivity field at each spatial point effectively partition phase space into zones of different particle fates, i.e., inertial particles initially located on either side of a ridge will evolve to different spatial locations after a short time. The phase space location of these ridges depends on the Stokes number, and by implication the size of the inertial particles of interest. This dependence can be exploited to make particles of different sizes cluster in different regions of the fluid and thus separate and segregate them.

We used this method to achieve segregation using a simple test model of two-dimensional flow: cellular flow. By “injecting” a mixture of inertial particles of different sizes into the fluid at a common relative velocity range that is sandwiched between the ridges of different Stokes number, the particles are segregated by size in a short time. Though we have based our results on only cellular flow, the methodology presented only requires that the underlying flow (1) has a spatial partition, i.e., separatrices in the fluid itself and (2) is of low Reynolds number. These requirements ensure

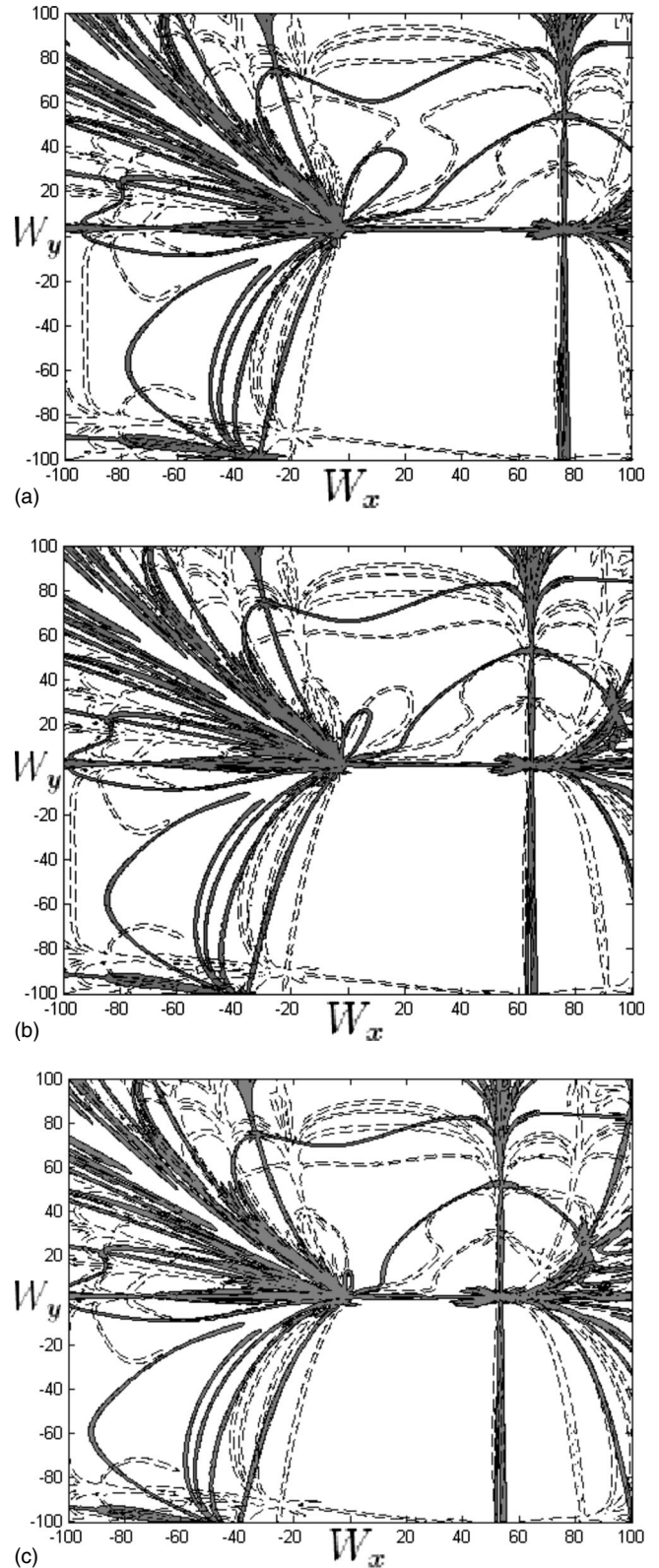


FIG. 5. (a) Ridges in the sensitivity field for the time-dependent stream function  $\psi(x,y,t) = a \cos(x + b \sin \omega t) \cos y$  for  $(x_0, y_0) = (3\pi/8, 3\pi/8)$ . The hatched and thick lines are the ridges corresponding to  $St=0.2$  and  $0.1$ , respectively. Parameters:  $a=100$ ,  $b=0.25$ ,  $\omega=1$ ,  $T=0.24$ . Initial times  $t_0=(a) 0$ ; (b) 0.25; (c) 0.5.

that segregated particles do not remix. The method does not rely on any other flow characteristic or specific stream function. Extending this to turbulent flows may present difficulties, since the ridges in the sensitivity field may not persist for long enough times to achieve a clean separation of the inertial particles. This aspect requires further investigation.

In future work, the approach employed here can be adapted to segregate non-neutrally-buoyant particles, and to segregate particles by other characteristics, e.g., density and shape, with a goal of designing flows that can fractionally separate particles for a range of inertial parameters.

- 
- [1] G. Segre and A. Silberberg, *Nature (London)* **189**, 209 (1961).  
 [2] M. Tirumkudulu, A. Tripathi, and A. Acrivos, *Phys. Fluids* **11**, 507 (1999).  
 [3] T. Shinbrot, M. M. Alvarez, J. M. Zalc, and F. J. Muzzio, *Phys. Rev. Lett.* **86**, 1207 (2001).  
 [4] S. A. Isard, S. H. Gage, P. Comtois, and J. H. Russo, *Bio-Science* **55**, 851 (2005).  
 [5] D. G. Schmale, A. S. Shah, and G. C. Bergstro, *Phytopathology* **95**, 472 (2006).  
 [6] M. C. Facchini, M. Mircea, S. Fuzzi, and R. J. Charlson, *Nature (London)* **401**, 257 (1999).  
 [7] E. R. Abraham, *Nature (London)* **391**, 577 (1998).  
 [8] T. Nishikawa, Z. Toroczkai, and C. Grebogi, *Phys. Rev. Lett.* **87**, 038301 (2001).  
 [9] A. Athanas and G. K. Johannes, *Chem. Eng. Technol.* **29**, 13 (2006).  
 [10] L. R. Huang, C. E. Cox, R. H. Austin, and J. C. Sturm, *Science* **304**, 987 (2004).  
 [11] J. A. Davis, D. W. Inglis, K. J. Morton, D. A. Lawrence, L. R. Huang, S. Y. Chou, J. C. Sturm, and R. H. Austin, *Proc. Natl. Acad. Sci. U.S.A.* **103**, 14779 (2006).  
 [12] D. DiCarlo, D. Irimia, R. G. Tompkins, and M. Toner, *Proc. Natl. Acad. Sci. U.S.A.* **104**, 48 (2007).  
 [13] M. R. Maxey and J. J. Riley, *Phys. Fluids* **26**, 883 (1983).  
 [14] M. R. Maxey, *Phys. Fluids* **30**, 1915 (1987).  
 [15] A. Babiano, J. H. E. Cartwright, O. Piro, and A. Provenzale, *Phys. Rev. Lett.* **84**, 5764 (2000).  
 [16] I. J. Benczik, Z. Toroczkai, and T. Tel, *Phys. Rev. Lett.* **89**, 164501 (2002).  
 [17] G. Haller and T. Sapsis, *Physica D* **237**, 573 (2008).  
 [18] G. Haller and T. Sapsis, *Phys. Fluids* **20**, 017102 (2008).  
 [19] J. Bec, *Phys. Fluids* **15**, L81 (2003).  
 [20] E. Balkovsky, G. Falkovich, and A. Fouxon, *Phys. Rev. Lett.* **86**, 2790 (2001).  
 [21] K. Duncan, B. Mehlig, S. Ostlund, and M. Wilkinson, *Phys. Rev. Lett.* **95**, 240602 (2005).  
 [22] J. Bec, *Phys. Fluids* **18**, 091702 (2006).  
 [23] I. J. Benczik, Z. Toroczkai, and T. Tel, *Phys. Rev. E* **67**, 036303 (2003).  
 [24] S. C. Shadden, F. Lekien, and J. Marsden, *Physica D* **212**, 271 (2005).  
 [25] F. Lekien, S. C. Shadden, and J. E. Marsden, *J. Math. Phys.* **48**, 065404 (2007).  
 [26] K. Ide, D. Small, and S. Wiggins, *Nonlinear Processes Geophys.* **9**, 237 (2002).